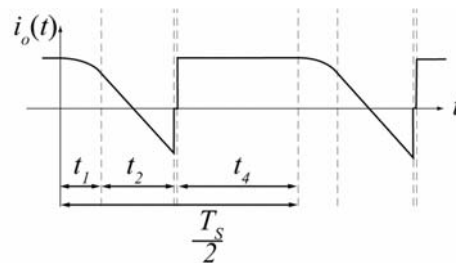
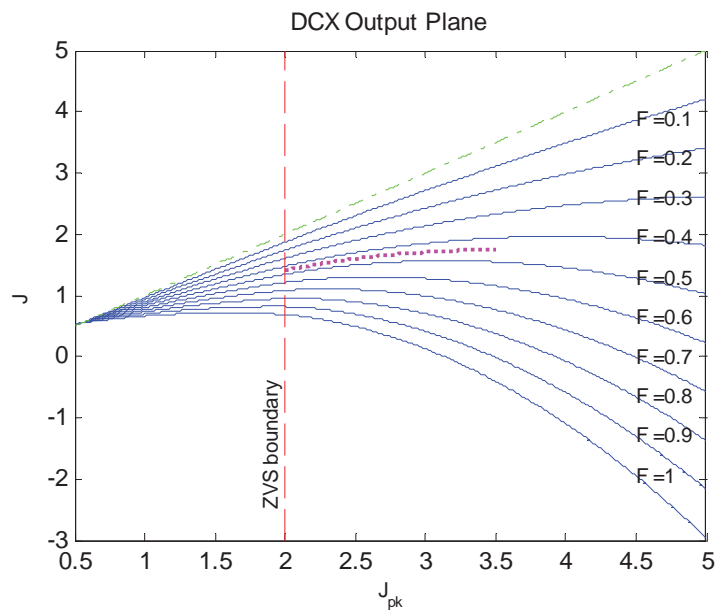


Averaging Step

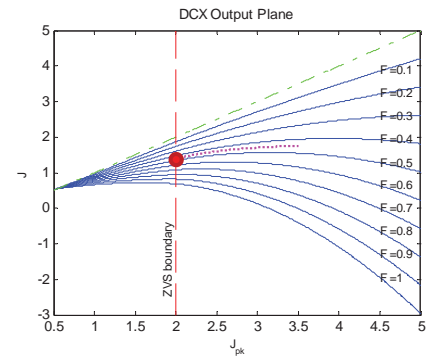
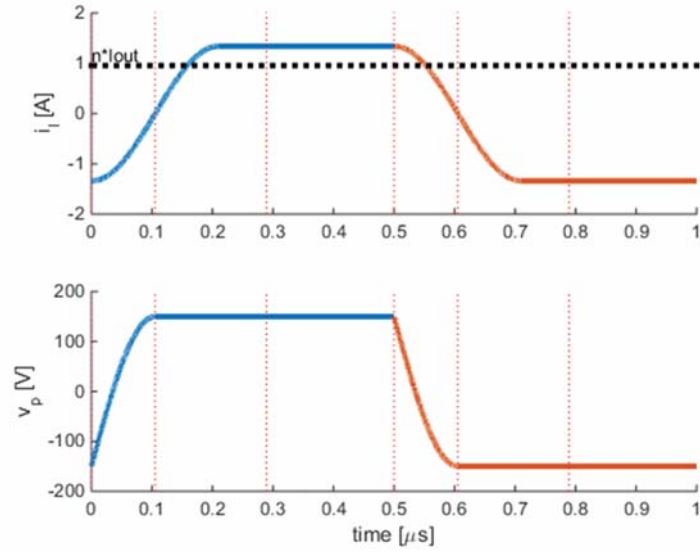


Output Plane

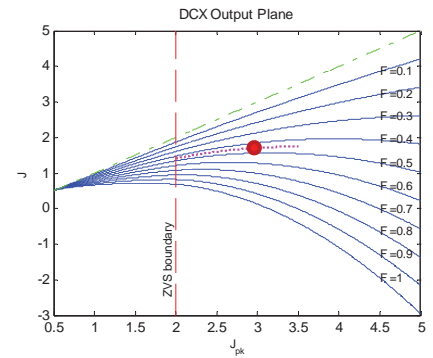
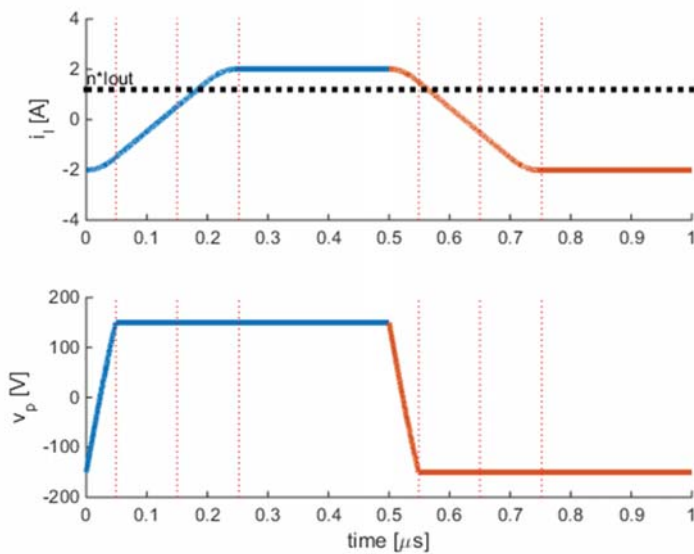
$$J = \frac{n \langle i_{out} \rangle}{I_{base}} = \frac{F}{\pi} \left[2 + \frac{1}{4} (J_1^2 - J_2^2) + J_p \left(\frac{\pi}{F} - \alpha - \beta - \delta \right) \right]$$



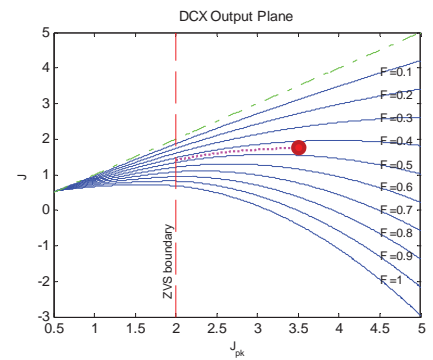
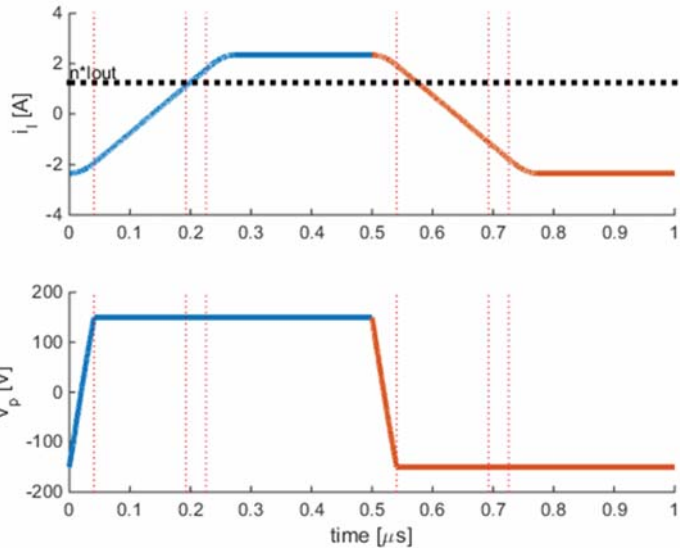
Example Waveforms



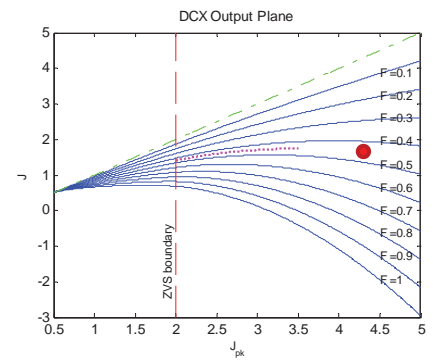
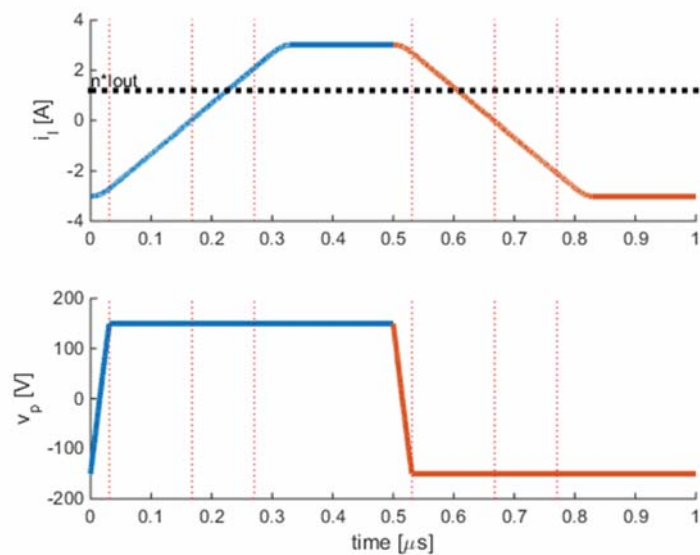
Example Waveforms



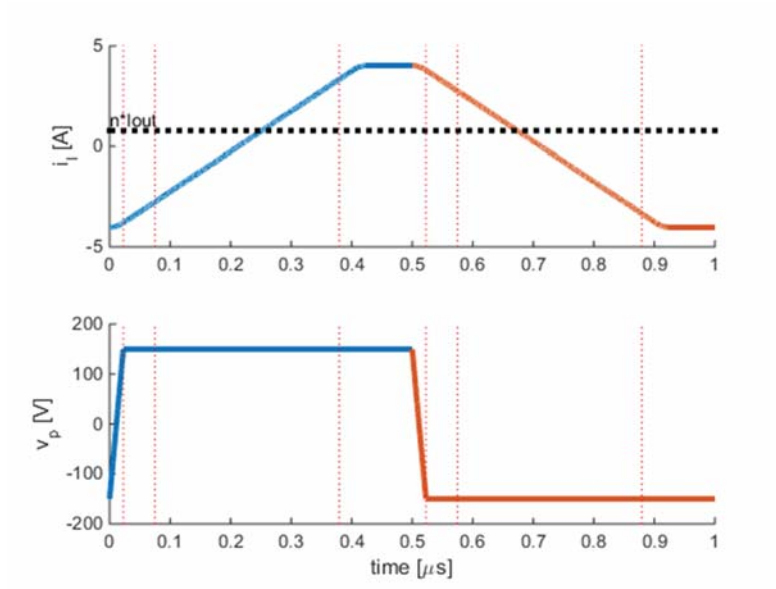
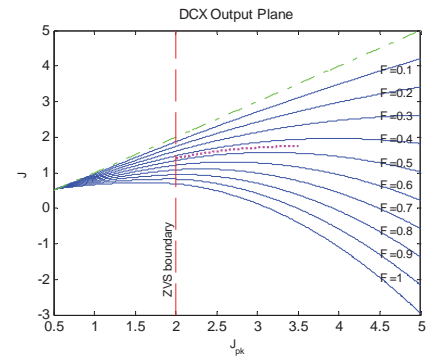
Example Waveforms



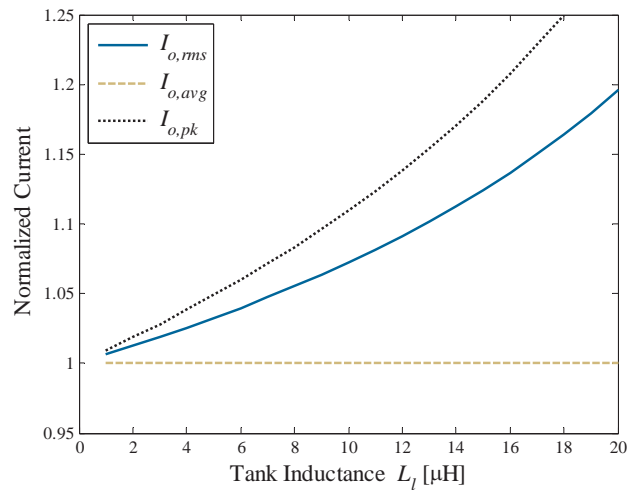
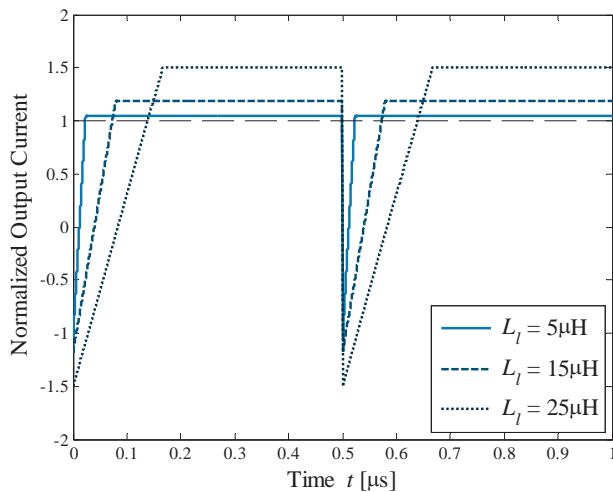
Example Waveforms



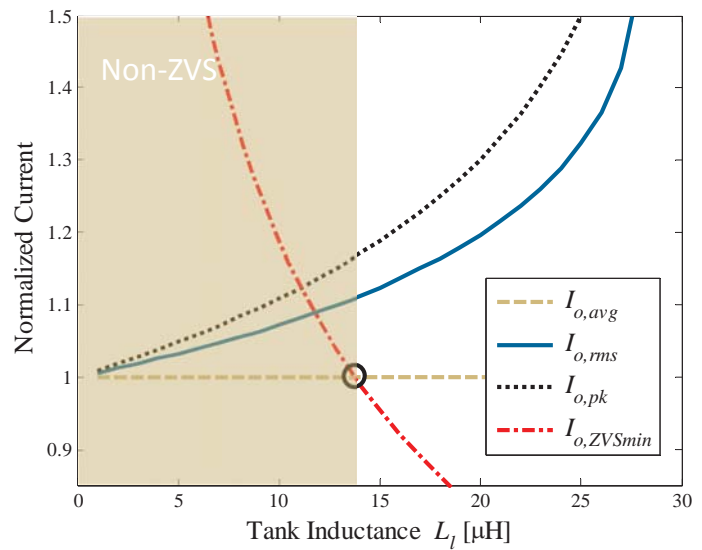
Example Waveforms



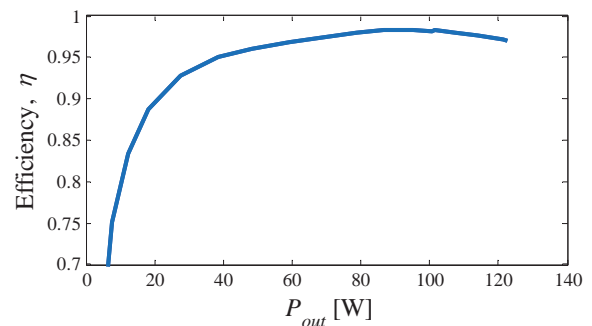
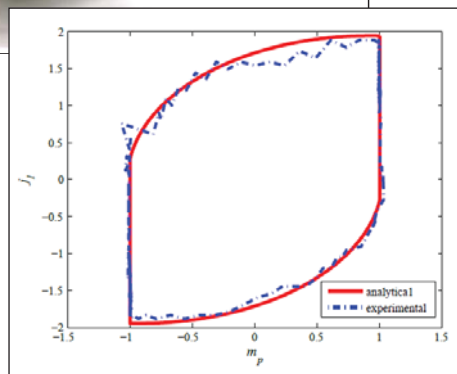
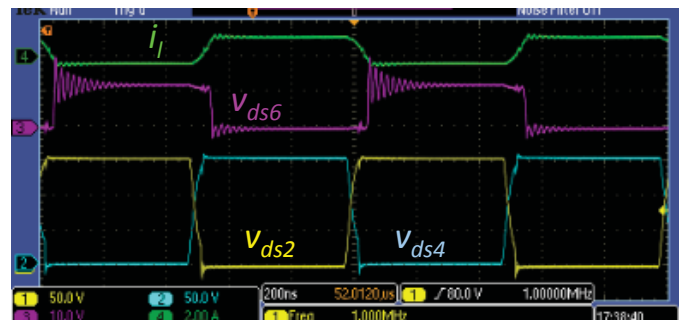
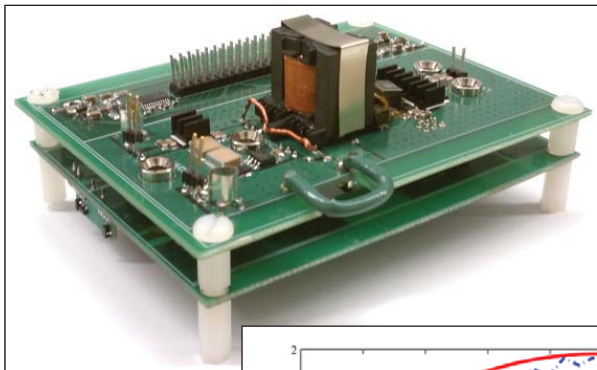
Output Current Vs. Inductance



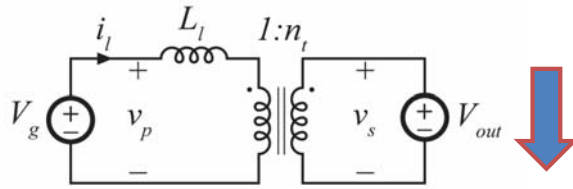
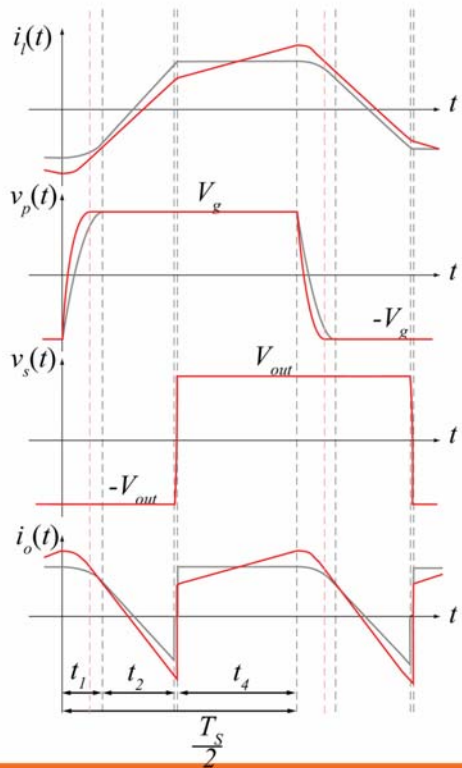
Constraints on Inductance



DAB: Experimental Results

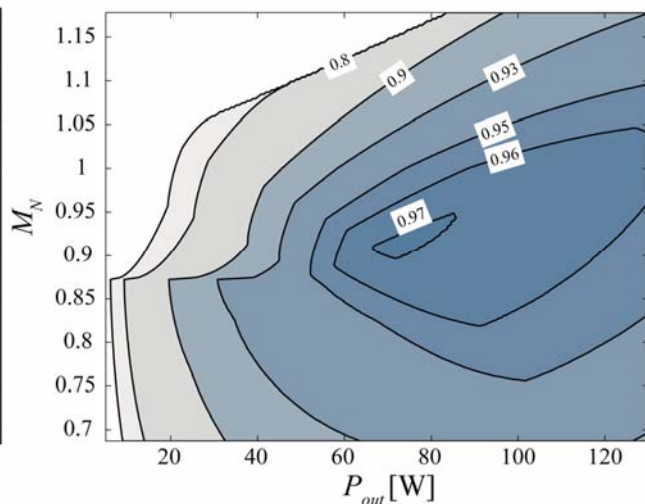
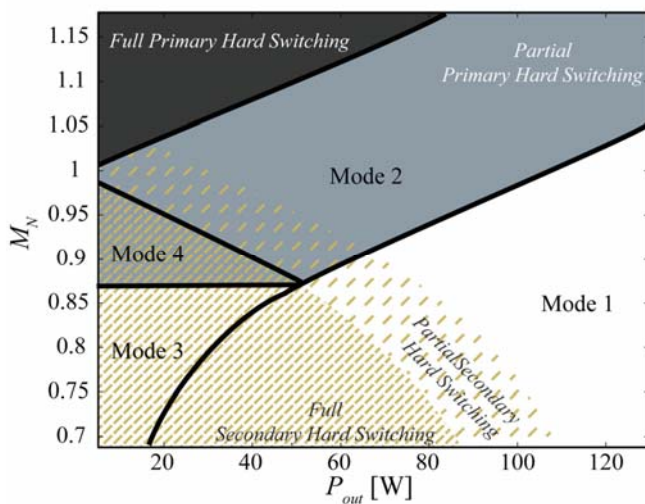


Operation with $V \neq nV_g$



- E.g. Decrease to $M_N < 1$ by decreasing output voltage
- Current now ramping, causing more energy available for primary ZVS, but higher RMS currents
- Can use behavior to extend ZVS range of one bridge

Soft Switching Range with Varying V_{out}



Application Example: Automotive

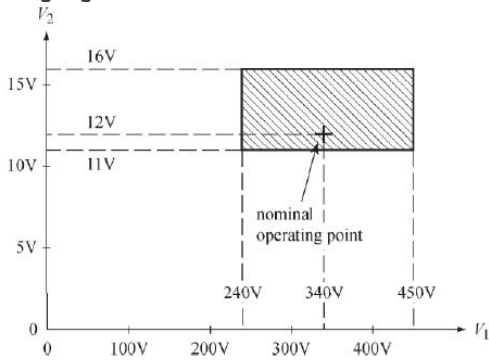


Fig. 1. Converter operating voltage ranges required for automotive application.

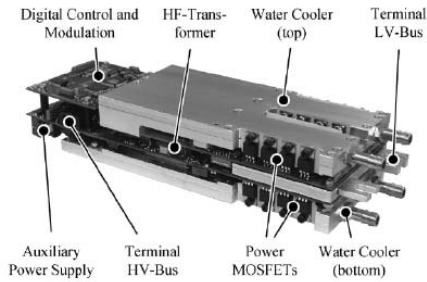


Fig. 3. Automotive DAB converter (273 × 90 × 53 mm).

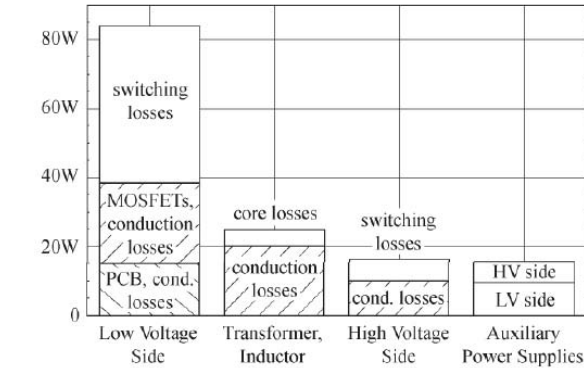
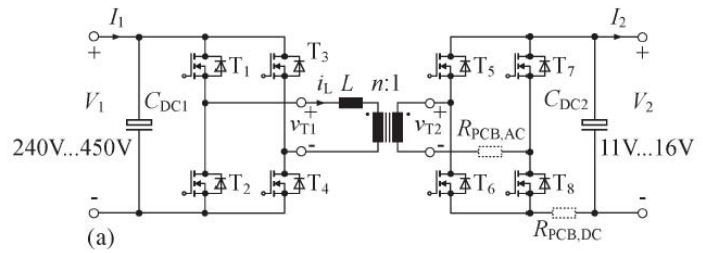


Fig. 13. Calculated distribution of the power losses for operation at $V_1 = 340$ V, $V_2 = 12$ V, and $P_2 = 2$ kW.

*F. Krismer, J.W.Kolar, "Accurate Power Loss Model Derivation of a High-Current Dual Active Bridge Converter for an Automotive Application, IEEE Trans. On Industrial Electronics, March 2010



Alternate Modulation Schemes

